



**HAL**  
open science

# The role of spatial heterogeneity in shaping pathogen populations in agricultural landscapes

Manon Couty, Florence Carpentier, Hervé Monod, Christian Lannou, Julien Papaïx

► **To cite this version:**

Manon Couty, Florence Carpentier, Hervé Monod, Christian Lannou, Julien Papaïx. The role of spatial heterogeneity in shaping pathogen populations in agricultural landscapes. 2024. hal-04695301

**HAL Id: hal-04695301**

**<https://hal.science/hal-04695301v1>**

Preprint submitted on 12 Sep 2024

**HAL** is a multi-disciplinary open access archive for the deposit and dissemination of scientific research documents, whether they are published or not. The documents may come from teaching and research institutions in France or abroad, or from public or private research centers.

L'archive ouverte pluridisciplinaire **HAL**, est destinée au dépôt et à la diffusion de documents scientifiques de niveau recherche, publiés ou non, émanant des établissements d'enseignement et de recherche français ou étrangers, des laboratoires publics ou privés.

# The role of spatial heterogeneity in shaping pathogen populations in agricultural landscapes

Manon Couty<sup>a</sup>, Florence Carpentier<sup>bc</sup>, Hervé Monod<sup>c</sup>, Christian Lannou<sup>d</sup>, Julien Papaïx<sup>a</sup>

<sup>a</sup>INRAE, BioSP, 84914 Avignon, France

<sup>b</sup>AgroParisTech, 75005, Paris, France

<sup>c</sup>INRAE, MaIAGE, 78352, Jouy-en-Josas, France

<sup>d</sup>INRAE, BIOGER, 78850, Thiverval-Grignon, France

**Summary:** Which pathogen genotypes will develop on which crop cultivar? This is a crucial question in plant epidemiology for understanding the link between the host population structure and its susceptibility to disease. In the present work, we develop a theoretical approach to investigate the conditions of emergence and establishment of a mutant pathogen with generalist features in an agricultural landscape, then we determine the conditions of co-existence between genotypes with specialist and generalist features. We found that the spatial structure of landscape heterogeneity had a strong effect on the genetic structure of the pathogen population. In particular, the geometry and size of the host genotype aggregates interacted with the initial position of inoculums to determine the ability of the generalist pathogen to establish locally. In addition, coexistence among generalist and specialist pathogen genotypes occurred rather easily while only two hosts are cultivated. We finally discuss the implication of our findings in a management perspective.

**Key words:** Population establishment, coexistence, spatial heterogeneity, landscape epidemiology

## 1. Introduction

The development of agriculture has accelerated adaptive phenotypic changes in pathogen populations (Palumbi, 2001; Hendry et al., 2008) leading to the emergence of new species (Stukenbrock et al., 2007; Gibbs et al., 2008) or to the differentiation and subsequent specialisation of sub-populations (Munkacsi et al., 2008; Gladieux et al., 2010). A well-documented example is that of the rice-infecting lineage of *Magnaporthe oryzae*, a fungal pathogen causing devastating epidemics in crops. *M. oryzae* emerged between 5000 and 7000 years BP following a host shift from *Setaria millet* to rice (Couch et al., 2005). In 1989, a host shift of the same pathogen from rice to wheat is assumed to have caused the emergence of wheat blast in Brazil. Such major events have been described for several crop pathogens (Stukenbrock and McDonald, 2008) and are probably unavoidable.

Although more discrete, pathogen specialisation to crop cultivars is much more common and causes the most popular cultivars to become increasingly susceptible to different diseases. Johnson (1961) used the term 'Man-guided' to describe how wheat selection for resistance during the 20th century, as well as growing practises, have shaped the *Puccinia* sp. populations, a group of pathogens causing the 'rust' disease on wheat. Breeding for resistance in cultivated plants has largely relied on the exploitation of the 'gene-for-gene' system (Flor, 1971). According to this system, avirulence genes in the pathogen are matched by resistance genes in the host. These 'qualitative resistance' genes confer immunity to the plant, which explains their popularity in breeding programs. They are however easily overcome by the pathogen after mutation or deletion of the avirulence gene and, in the recent past, the release of resistant cultivars has usually led to the adaptation of pathogen populations through accumulation of qualitative pathogenicity factors. A very demonstrative example can be found by comparing

the French populations of *Melampsora larici-populina*, a pathogen causing poplar rust, on wild and cultivated host populations (Gérard et al., 2006).

The evolution of crop pathogens driven by the ‘gene-for-gene’ system has been largely documented (Wolfe and Schwarzbach, 1978; Hovmoller et al., 1993; Rouxel et al., 2003; Goyeau et al., 2006; Barrès et al., 2008) but is not sufficient to explain the high specialisation level that is observed in those pathogens. Based on a large database analysis coupling pathogen frequency data and disease observation data, Papaïx et al. (2011) showed that pathogen specialisation in crops is largely accounted for by quantitative pathogenicity. Indeed, selection for quantitative traits influences pathogen evolution in agricultural systems and can result in differential adaptation to host genotypes (Pariaud et al., 2009; Lannou, 2012). Such differential adaptation of pathogen genotypes to host genotypes largely accounts for the relationship between the composition of the host population and its susceptibility to disease (Papaïx et al., 2011). Which pathogen genotypes will develop on which crop cultivar? is thus a crucial question in plant epidemiology for understanding the link between the host population structure and its susceptibility to disease. This question required the understanding of coexistence mechanisms in heterogeneous environments.

The first condition for a new pathogen genotype to maintain in a population is success in establishment of a population (With, 2002). In homogeneously mixed host-pathogen systems establishment success is determined by the pathogen basic reproductive number ( $R_0$ ). When two pathogens are competing for a single host genotype, the pathogen with the highest  $R_0$  will invade the resident population. However, when dispersal is limited, the pathogen population will typically progress in a susceptible host population as a travelling wavefront (Mundt et al., 2009). In such conditions, a mutant genotype will be overwhelmed if it appears in the already diseased region and it will become more likely established if it arises closer to the wavefront (Wei and Krone, 2005). This effect is known as the ‘surfing effect’ in population genetics

(Excoffier and Ray, 2008). The effects of landscape structure on the establishment of a mutant have been rarely investigated in the literature. Burton and Travis (2008) constructed a model for simulating the expansion range of haploid individual. They found that landscape structure together with the spatial location of mutant introduction have a considerable influence on the mutant survival probability and on the population dynamics of the mutants. In particular the landscape structure could favour deleterious mutations that would normally disappear.

When all genotypes are established in the population, the question of stable coexistence can be addressed. A classical mechanism for coexistence is niche partitioning (Chesson, 2000). This requires that genotypes differ in their use of resources but not necessarily that these resources fluctuate in space (homogeneous environment). Environment heterogeneity makes however easier a stable coexistence because it promotes mechanisms that are not possible in homogeneous environments (Melbourne et al., 2007). Chesson (2000) identified three mechanisms that depend on the variation of resources in space: storage effect, relative non-linearity and fitness-density covariance. More recently, Débarre and Lenormand (2011) added another mechanism: ‘habitat boundary polymorphism’. This mechanism requires both habitat heterogeneity and distance-limited dispersal, which creates maladaptation of specialists at habitat edges and favour the maintenance of more generalist genotypes.

However, while these theoretical considerations help understanding general mechanisms of species coexistence, epidemiological models at the scale of agricultural landscapes are still needed to understanding consequences of crop deployment strategies on pathogen population structure and disease severity. We developed a spatially explicit stochastic model based on an air-borne plant-pathogen foliar fungus. The landscape is represented as a set of fields on which two crop cultivars are deployed with controlled proportion and spatial organisation. We consider also several dispersal abilities and several specialisation costs for the pathogen. We consider two case-studies: (i) the establishment of a generalist population during the spread of

the pathogen population composed of two specialised genotypes; (ii) the stable coexistence among the three pathogen genotypes.

## **2. Materials and methods**

### **2.1. Spatial structure**

5 field patterns composed of around 155 fields were generated by simulating a set of crop fields using a T-tessellation algorithm that made it possible to control the size, number and shape of fields (Kiêu et al., 2013; Papaix et al., 2014). Then, each field was divided into patches by intersecting a regular grid with the field pattern to account for intra-field dispersal. The patch was then the spatial unit of the system: the pathogen population was supposed to be perfectly mixed at the patch level and it dispersed within and among patches.

Two crop cultivars,  $V_1$  and  $V_2$ , were deployed on each field pattern with controlled spatial arrangements defined by their proportions in surface coverage (10%, 30% and 50% of the cultivar  $V_1$ ) and landscape aggregation level. Local aggregation was first defined as the proportion of neighbour fields that shared the same host type. Here, two fields were considered as neighbours if they shared a common edge. The landscape aggregation level is then the mean of local aggregation over the landscape. We defined 3 landscape aggregation levels: mixed (low landscape aggregation), mosaic (medium landscape aggregation) and clustered (high landscape aggregation – Figure 1). For each combination of field pattern, variety proportion and aggregation, two landscape replicates in the allocation of cultivars were obtained by means of a simulated annealing algorithm.

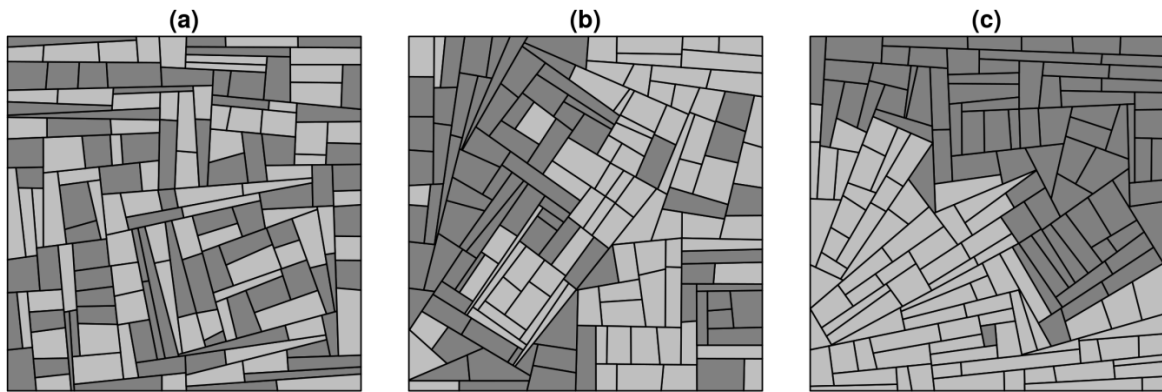


**Figure 1:** Examples of simulated landscapes with a balanced cropping ratio and an increasing global aggregation (from a to c, mixed, mosaic and clustered).

**Table 1:** Definitions of the main terms and parameters used in modelling.

Symbols	Description	Value
<i>1) Landscape spatial structure</i>		
-	Number of fields	155, 154, 152, 153 and 156
-	Number of crop varieties	2
-	Cropping ratio	10%-90%, 30%-70% and 50%-50%
-	Aggregation among the varieties	3 scenarios: mixed, mosaic and clustered
<i>2) Pathogen dispersal</i>		
$\mu_0$	Mean dispersal distance	2.5, 10 and 25% of the landscape scale
$a$	Weight of the dispersal tail	3.4
<i>3) Life-history traits</i>		
	Spore production	2 by infected site by day
	Infection efficacy	From 0.04 to 0.15 depending on the host and pathogen genotype
	Latent period	5
	Infectious period	10
	Mutation rate	$10^{-5}$
	Host growth rate	0.1

## 2.2. Population dynamics model

### 2.2.1. Overview

We developed a Susceptible-Expected-Infectious-Removed (SEIR) model with spores as a propagule state. The pathogen population was composed of 3 genotypes,  $P_1$ ,  $P_2$  and  $P_3$ .  $P_1$  and  $P_2$  were both specialists of cultivars  $V_1$  and  $V_2$ , respectively, whereas  $P_3$  had generalist features and perceived the landscape as homogeneous. Each patch was considered as a set of infection sites (here after denominated only by “site”) with no spatial positions. The model described the dynamics of the number of sites in each of the following states and for each patch  $i$ : healthy sites ( $S_i$ ), latent sites infected by the pathogen genotype  $p \in \{P_1, P_2, P_3\}$  ( $E_{i,p}$ ), infectious sites infected by the pathogen genotype  $p$  ( $I_{i,p}$ ) and removed sites previously infected by the pathogen genotype  $p$  ( $R_{i,p}$ ). We described below each step of the model according to their chronology. Parameters are summarized in Table 1.

### 2.2.2. Reproduction and mutations

Infectious sites produced  $r = 2$  effective spores per day resulting from the real number of produced spores and the leaf frailty (Soubeyrand et al., 2007). Spores belonged to the same genotype as their parental lesion with probability  $m_{pp}$ . We assumed that mutations from genotype  $p$  to genotype  $p'$  ( $p \neq p'$ ) arose with probability  $m_{pp'}$ . In patch  $i$  and time  $t$ , the number of spores of type  $P_1$ ,  $P_2$  and  $P_3$  produced by the pathogen genotype  $p$ ,  $M_{i,p}(t)$ , write:

$$M_{i,p}(t) \sim \text{Multi}(rI_{i,p}(t-1), [m_{pp_1}, m_{pp_2}, m_{pp_3}]).$$

Thus, the total number of spores,  $Sp_{i,p}(t)$ , belonging to the pathogen genotype  $p$  and produced in patch  $i$  and time  $t$  was computed as  $Sp_{i,p}(t) = \sum_{p'} [M_{i,p'}(t)]_p$ .



### 2.2.3. Spores dispersal

Spores migrated from patch  $i$  to patch  $j$  with probability  $\mu_{i,j}$  computed from:

$$\mu_{i,j} = \frac{\int \int_{A_i A_j} g(\|z - z'\|) dz dz'}{A_i},$$

where  $A_i$  and  $A_j$  were the areas of patches  $i$  and  $j$ , respectively (Bouvier et al., 2009).

$g(\|z - z'\|)$  is the individual dispersal function with an inverse power law shape:

$$g(\|z - z'\|) = \frac{(a-2)(a-1)}{2\pi b^2} \left(1 + \frac{\|z - z'\|}{b}\right)^{-a},$$

where  $\|z - z'\|$  was the Euclidean distance between locations  $z$  and  $z'$ ,  $b > 0$  was a scale parameter and  $a > 2$  determined the weight of the dispersal tail.  $a$  was fixed to 3.4 to have a fat tailed dispersal function. The mean dispersal distance was defined only when  $a > 3$  as  $\mu_0 = 2b/(a-3)$ .

$[D_p(t)]_{i,j}$ , the element in the row  $i$  and column  $j$  of the dispersal matrix  $D_p(t)$  gives the number of spores of type  $p$  dispersing at time  $t$  from patch  $i$  to patch  $j$ :

$$[D_p(t)]_{i,\bullet} \sim \text{Multi}(Sp_{i,p}(t), [\mu_{i,1}, \mu_{i,2}, \dots]).$$

Thus, the total numbers of spores of type  $p$  ( $Sp_{j,p}^{tot}(t)$ ) arriving in patch  $j$  at time  $t$  were computed as  $Sp_{j,p}^{tot}(t) = \sum_i [D_p(t)]_{i,j}$ .

### 2.2.4. Contamination of susceptible sites

Spores arriving on a patch contaminated a susceptible site with probability

$$\pi(x) = 1 - \frac{\exp(-\kappa x^\sigma) - \exp(-\kappa)}{1 - \exp(-\kappa)}, \text{ with parameters } \kappa > 0 \text{ and } \sigma \geq 0. \text{ Thus } \pi(\cdot) \text{ decreases with}$$

epidemic development as healthy sites become rarer. The function  $\pi(\cdot)$  insures that contamination is certain ( $\pi(1) = 1$ ) if all sites are healthy and impossible ( $\pi(0) = 0$ ) if there are

no healthy sites. The number of new possible infections (spores that entered in contact with a susceptible site),  $NewCont_i(t)$ , in patch  $i$  and time  $t$  was first computed regardless the pathogen genotype as:

$$NewCont_i(t) \sim \text{Bin}(S_i(t-1), \pi(x_i(t-1))).$$

Then, the new possible infections were dispatched among the pathogen genotypes according to their proportion in the set of spores arriving in the patch  $i$  and time  $t$  and following a multinomial distribution:

$$[NewContP_{i,p_1}(t), NewContP_{i,p_2}(t), NewContP_{i,p_3}(t)] \sim \text{Multi} \left( NewCont_i(t), \left[ \frac{Sp_{i,p}^{tot}(t)}{\sum_{p'} Sp_{i,p'}^{tot}(t)} \right]_{p \in \{p_1, p_2, p_3\}} \right)$$

Note that the actual number of spores arriving on a patch was taken as a maximum for new possible infections.

### 2.2.5. Infection of susceptible sites

A susceptible site receiving a spore (contaminated site) became infected with a probability  $e_{p,v(i)}$ , the infection efficacy of pathogen genotype  $p$  on the crop variety  $v(i)$  cultivated in patch  $i$ . We thus have:

$$NewE_{i,p}(t) \sim \text{Bin}(NewContP_{i,p}(t), e_{p,v(i)}).$$

### 2.2.6. Transition from latent (E) to infectious (I) sites

Once infected, the site remained on average latent during  $\tau = 5$  days before becoming infectious. The transition from latent to infectious site was given by:

$$\begin{cases} NewI_{i,p}(t) \sim \text{Bin}(E_{i,p}(t-1), 1 - \exp(-1/\tau)) \\ E_{i,p}(t) = E_{i,p}(t-1) + NewE_{i,p}(t) - NewI_{i,p}(t) \end{cases}$$

### 2.2.7. Removal of infectious hosts

After an average  $T = 10$  days of sporulation (infectious period), the infectious site was removed. The transition from infectious site to removed site was given by:

$$\begin{cases} \text{New}R_{i,p}(t) \sim \text{Bin}\left(I_{i,p}(t-1), 1 - \exp\left(-\frac{1}{T}\right)\right) \\ I_{i,p}(t) = I_{i,p}(t-1) + \text{New}I_{i,p}(t) - \text{New}R_{i,p}(t) \end{cases}$$

### 2.2.8. Host growth and removal of infected hosts

In patch  $i$ , the host grew locally until it reached the carrying capacity of that patch,  $K_i$ , where  $K_i$  was assumed to be proportional to the area of patch  $i$ . In addition, we considered that only green tissues (i.e. susceptible sites  $S_i$ ) participated to biomass production (equivalent to a castrating pathogen):

$$\begin{cases} \text{New}S_i(t) \sim \text{Bin}\left(S_i(t-1), \delta \left(1 - \left(S_i(t-1) + \sum_p E_{i,p}(t-1) + \sum_p I_{i,p}(t-1)\right) / K_i\right)\right) \\ S_i(t) = S_i(t-1) + \text{New}S_i(t) - \sum_p \text{New}E_{i,p}(t) \end{cases}$$

where  $\delta$  is the intrinsic rate of biomass production.

## 2.3. Numerical experiments

### 2.3.1. Case studies

We first investigated the establishment of a generalist population. The generalist genotype  $P_3$  was assumed to be continually introduced by mutation of specialist genotypes  $P_1$  and  $P_2$  ( $m_{P_1P_3} = m_{P_2P_3} = 10^{-5}$ ). Because foundation effects could be of prime importance in the establishment phase, we assumed no growth of the host ( $\delta = 0$ ) and ran the simulation until all sites were occupied by the pathogen. We started the epidemic with 20 infectious sites (10 of  $P_1$

and 10 of  $P_2$ ) on a randomly chosen  $V_1$  patch, and 20 infectious sites (10 of  $P_1$  and 10 of  $P_2$ ) on a randomly chosen  $V_2$  patch.

We then investigated the coexistence among the three genotypes. We assumed that all genotypes pre-existed in the population and studied the composition of the pathogen population at equilibrium. Mutation rates were set to 0 and the host was assumed to grow continuously ( $\delta = 0.1$ ). Epidemics started with 30 infectious sites of each genotype in all patches.

### ***2.3.2. Life history traits***

Each specialist was confronted to a susceptible cultivar on which it benefited from a highest infection efficacy than the generalist (specialization gain) and a resistant cultivar on which it suffered from a lower infection efficacy than the generalist (specialization cost). Thus, with regards to the genotype  $P_1$ ,  $V_1$  was the susceptible cultivar and  $V_2$  was the resistant cultivar. Infection efficacy of the generalist genotype  $P_3$  was fixed to 0.1. For the specialist genotypes, infection efficacy on their susceptible cultivars ( $e_S = e_{P_1, V_1} = e_{P_2, V_2}$ ) varied from 0.11 to 0.15 by 0.01 whereas infection efficacy on their resistant cultivars ( $e_R = e_{P_1, V_2} = e_{P_2, V_1}$ ) varied from 0.04 to 0.09 by 0.01.

We assessed the role of the mean dispersal distance by varying  $\mu_0$  equal to 2.5%, 10% and 25% of the landscape scale.

For all of the 90 cross combinations of infection efficacy and mean dispersal distance 5 field patterns  $\times$  2 landscape replicates  $\times$  2 model replicates = 20 simulations were performed.

## **2.4. Outputs and statistical analysis**

### ***2.4.1. Establishment of a generalist population***

The capacity of the generalist pathogen genotype  $P_3$  to establish a population was assessed by computing its frequency in the total pathogen population at the end of the epidemic spread.

In addition, to characterize whether its population was diffuse across the landscape or more localized we computed the maximal frequency that  $P_3$  reached in a field. Due to highly non-linear responses, these two output variables were analyzed by means of generalized additive models (gam) with tensor product smoothers using the package mgcv (Wood, 2011) of the R software (R Core Team, 2018). The explanatory variables were variables describing the landscape configuration (landscape aggregation level and cropping proportion) and quantitative variables describing the pathogen traits (pathogen dispersal, infection efficacies of specialized genotypes for their resistant and susceptible varieties)

Finally, we investigated in more details how local spatial structures in the host population allowed local establishment of  $P_3$  by studying the relationship between the intra-field proportion of  $P_3$  and the local aggregation of crop varieties. This was done by means of a linear mixed model in the R software, with local aggregation and global variety proportion (quantitative variables) and their interactions with landscape aggregation levels as fixed effects, and the landscape as random effect.

#### ***2.4.2. Coexistence among pathogen genotypes***

Coexistence among the three pathogen genotypes was investigated by classifying the simulations into possible outcomes of genotype persistence. A given genotype persisted in the pathogen population if its global proportion (infectious sites) was greater than 5%. Simulations were then analyzed by fitting a multinomial regression model using the package nnet (Venables and Ripley, 2002) of the R software.

In addition, we studied spatial patterns in pathogen diversity at equilibrium. We computed genotype frequencies (infectious sites) at the field scale by averaging the values of the intra-field patches and investigated how they were related to the local configuration of the crop cultivars. This was done by means of a linear mixed model in the R software, with global

aggregation, local aggregation and proportion as fixed effects, and the landscape as random effect.

### 3. Results

#### 3.1. Establishment of a population

The proportion of simulations leading to the establishment of a  $P_3$  population dropped quickly as the cost the specialists suffered on their resistant host decreased and the gain they benefited on their susceptible host increased. In fact, 53.1% of the simulations led to the establishment (*i.e.* the total pathogen population was composed of more than 1% of  $P_3$ ) of a  $P_3$  population when  $e_R=0.04$  and  $e_S=0.1$ , but only 13.1% and 0.2% of the simulations led to the establishment of a  $P_3$  population when  $e_R=0.05$  and  $e_S=0.12$  or when  $e_R=0.06$  and  $e_S=0.13$ , respectively. Below we only discuss the case when  $e_R=0.11$  and  $e_S=0.04$ . In the other cases, the general conclusions were the same but with a lower proportion of  $P_3$ .

Landscape aggregation level of crop varieties was crucial to determine the ability of  $P_3$  to establish a population, with mixed landscapes favoring the highest proportion of  $P_3$  in the pathogen population across the landscape (Figure 2). In mixed landscapes,  $P_3$  cannot get established for a low pathogen mean dispersal distance when the cropping ratio was balanced whereas, for a high pathogen mean dispersal distance,  $P_3$  cannot get established when the cropping ratio of one of the two cultivars was low. Otherwise, the proportion of  $P_3$  in the pathogen population increased with increases in pathogen mean dispersal distance and proportion of  $V_1$  (until the cropping ratio became balanced). In mosaic landscapes (medium landscape aggregation), the highest proportions of  $P_3$  were obtained only for a high mean

dispersal distance and around 30% of  $V_1$ . The generalist was not able to establish a population when the variety aggregation was at its maximum.

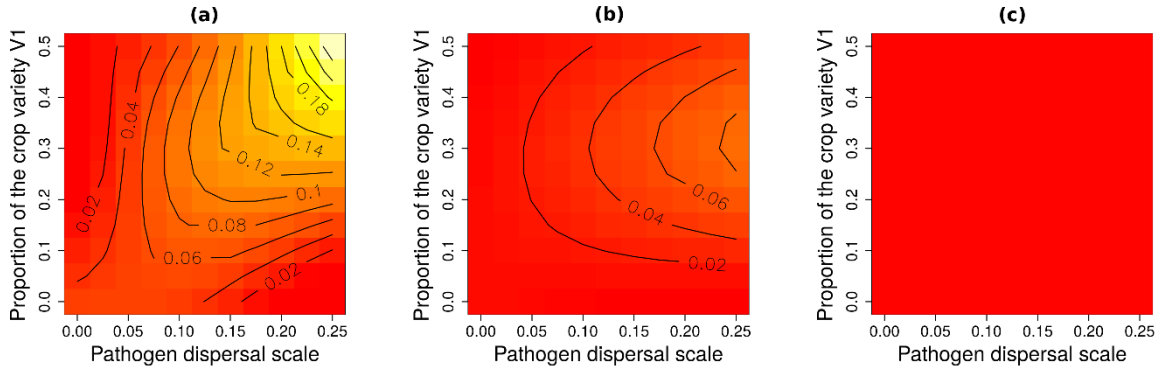


**Figure 2:** Predicted frequency of the generalist pathogen genotype at the landscape scale as a function of cropping ratio and pathogen dispersal scale in the 3 levels of landscape aggregation (a, mixed ; b, mosaic ; c, clustered). These response surfaces were obtained using the generalized additive models estimated on the simulations corresponding to  $e_{P_1,V_1} = e_{P_2,V_2} = 0.11$  and  $e_{P_1,V_2} = e_{P_2,V_1} = 0.04$ . Note that the homogenous red colour in panel c corresponds to predicted frequencies inferior at 0.02.

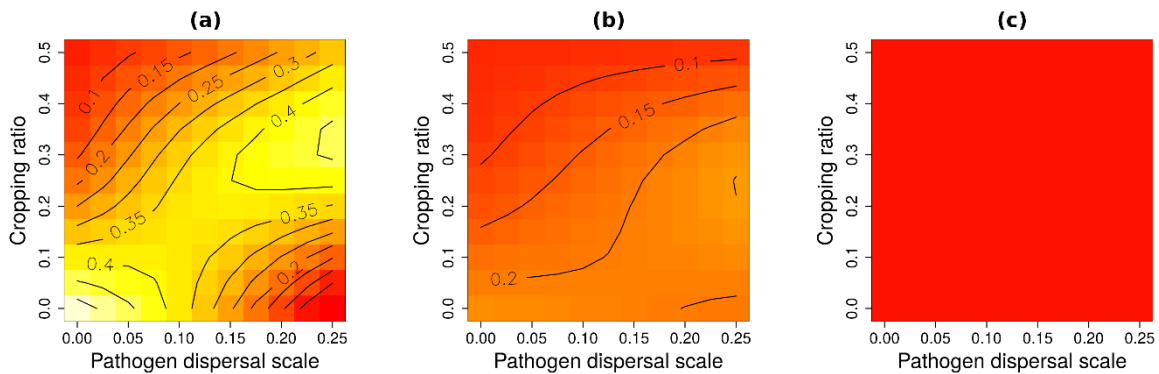


**Figure 3:** Predicted maximal frequency of the generalist pathogen genotype in the landscape as a function of cropping ratio and pathogen dispersal scale in the 3 levels of landscape aggregation (a, mixed ; b, mosaic ; c, clustered). These response surfaces were obtained using the generalized additive models estimated on the simulations corresponding to  $e_{P_1,V_1} = e_{P_2,V_2} = 0.11$  and  $e_{P_1,V_2} = e_{P_2,V_1} = 0.04$ . Note that the homogenous red colour in panel c corresponds to predicted frequencies inferior at 0.02.

The maximal frequency that  $P_3$  reached locally responded generally in the same way that for the average  $P_3$  proportion across the landscape (Figure 3). However,  $P_3$  could reach a high frequency in the local pathogen populations even if it was not at its highest possible proportion

across the landscape, indicating that  $P_3$  could form highly concentrated and spatially limited populations. In mixed landscapes this was the case for low proportions of  $V_1$  and low mean dispersal distances or for high mean dispersal distances and around 30% of  $V_1$ . The ratio between maximal frequency and average  $P_3$  proportion is lower in mixed landscapes than in mosaic ones where the local frequency of the generalist could reach around 20% of the local pathogen population even though it was present only 2% at the landscape scale.

The role of the landscape and local spatial structures in favoring the establishment of local  $P_3$  populations was further investigated by studying the proportion of  $P_3$  at the field scale against the landscape and local aggregations of the crop varieties (Table 2). The intra-field proportion of  $P_3$  significantly decreased with the landscape aggregation level and with the landscape proportion of  $V_1$ . This effect is not significant in clustered landscape. The proportion of  $P_3$  at the field scale also decreased with the local aggregation (Figure 4), significantly in mosaic and clustered landscapes but not significantly in mixed landscapes. In addition, as the landscape aggregation level increased, the effect of local spatial structures (*i.e.* local aggregation) on local establishment of  $P_3$  increased whereas the effect of global landscape metrics (*i.e.* cropping ratio) decreased. Altogether, these results suggested that in mosaic and clustered landscapes, the generalist preferentially established in the most heterogeneous zones of the landscapes whereas in mixed landscapes,  $P_3$  established opportunistically in the landscape as it found a field that was not already colonized by the corresponding specialist. However, in mosaic landscapes, the highest proportions of  $P_3$  were observed in local aggregates of  $V_1$  (Figure 4). Such landscapes have complex spatial structures forming corridors, barriers and aggregates of crop varieties. These particular structures have the potential to hamper the spread of one of the specialists giving more chances for the generalist to establish



a population at the population front. This could explain the highest proportions of  $P_3$  observed in locally high aggregated area (Figure 4).

**Table 2:** Regression of intra-field proportion of  $P_3$  against the global fragmentation of the landscape, the proportion of variety  $V_1$  and the local aggregation of crop varieties.

Effect		Estimate	Standard Error	DF	t-value	p-value
	<b>Landscape aggregation level</b>					
<b>Landscape aggregation level</b>	Mixed	-0.60	0.25	84	-2.37	0.020
	Mosaic	-2.1	0.25	84	-8.32	0.0
	Clustered	-4.0	0.25	84	-15.6	0.0
<b>Local aggregation level</b>	Mixed	-0.20	0.17	8526	-1.16	0.25
	Mosaic	-1.9	0.057	8526	-33.1	0.0
	Clustered	-2.5	0.055	8526	-45.2	0.0
<b>Proportion of <math>V_1</math></b>	Mixed	-4.1	0.76	84	-5.40	0.0
	Mosaic	-1.7	0.74	84	-2.26	0.027
	Clustered	-0.25	0.74	84	-0.340	0.73

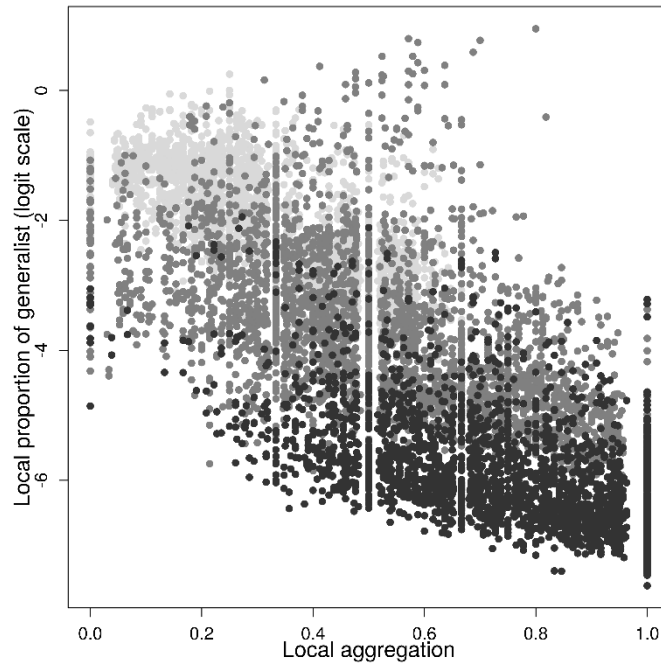


**Figure 4:** Local proportion of the generalist pathogen (logit scale) plotted against local aggregation for mixed (light grey), mosaic (dark grey) and clustered (black) landscapes. The displayed simulations correspond to  $e_{P_1, V_1} = e_{P_2, V_2} = 0.11$ ,  $e_{P_1, V_2} = e_{P_2, V_1} = 0.04$ , a dispersal scale equal to 0.1, and the establishment case study.

### 3.2. Coexistence among pathogen genotypes

Generally, specialists were at their advantage when their susceptible cultivar was well represented in the landscape, the dispersal ability was not too high and the spatial aggregation not too low. As the dispersal ability increased or the cropping ratio became more balanced, the generalist genotype was able to persist and even to outcompete the specialists particularly in mixed landscapes (Figure 5).

Interestingly, the coexistence among the three genotypes was easily observed across the simulations (Figure 5). To coexist, the genotypes required both variety aggregates to allow the specialists to persist together with heterogeneous zones where the generalist was at its advantage (Figure 6). This was the case in mosaic landscapes and coexistence was a common output that was also stable to variation in specialization cost and gain. In clustered landscapes coexistence among the three genotypes was also observed but was extremely sensitive to the specialization gain: as soon as the specialization gain increased the generalist did not persist anymore.

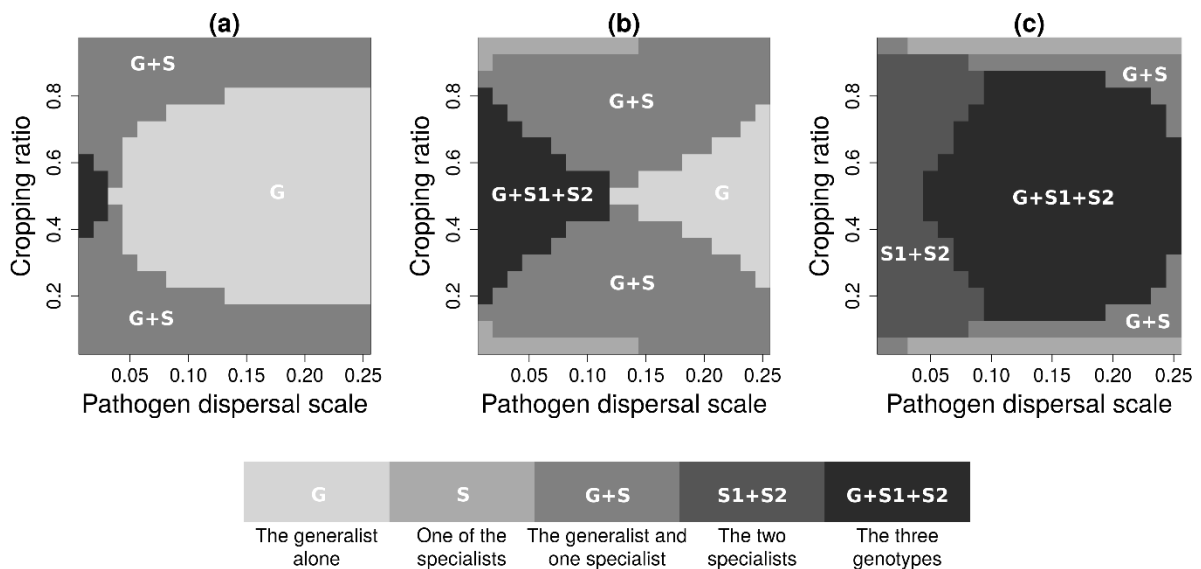


**Figure 5:** Predicted coexistence among the pathogen genotypes obtained by means of the multinomial regression in mixed (a), mosaic (b), and clustered (c) landscapes. Other parameters are:  $e_{P_1, V_1} = e_{P_2, V_2} = 0.11$  and  $e_{P_1, V_2} = e_{P_2, V_1} = 0.04$ .

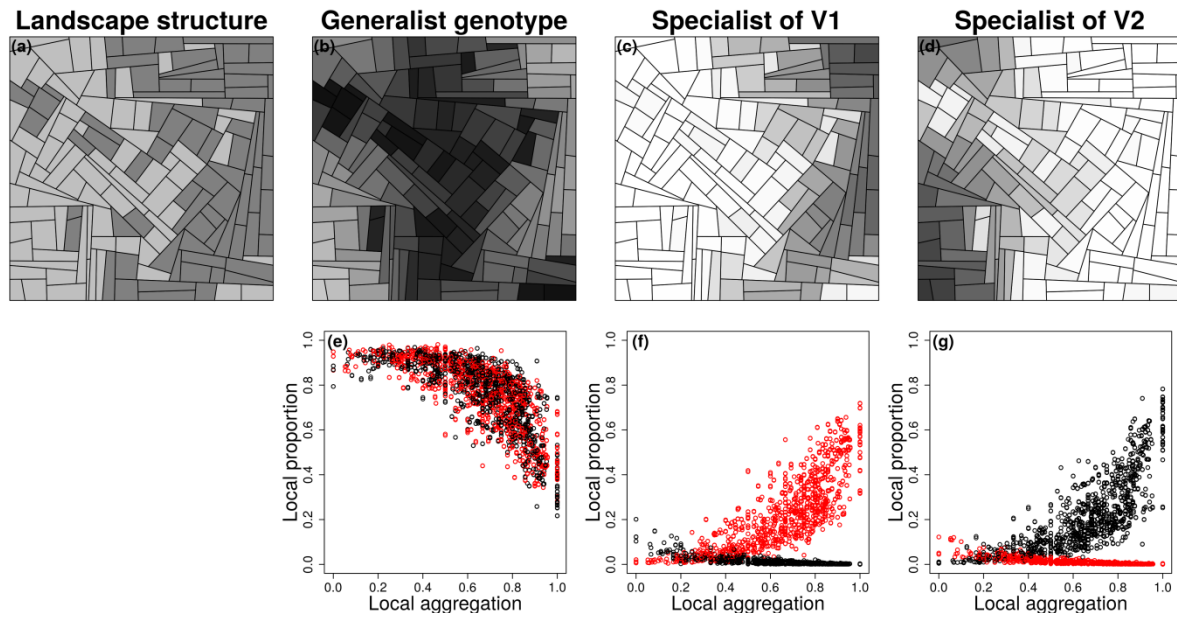


**Figure 6:** An example of a simulation where the three pathogen genotypes coexist. (a) Landscape structure (dark grey, variety  $V_1$ ; light grey variety  $V_2$ ). (b-d) spatial repartition of the generalist ( $P_3$ ), the specialist of variety  $V_1$  ( $P_1$ ) and specialist of variety  $V_2$  ( $P_2$ ), respectively. The grey scale represents the proportion of each genotype and range from 0 (white) to 1 (black). (e-g) intra-field proportion of the generalist ( $P_3$ ), the specialist of variety  $V_1$  ( $P_1$ ) and specialist of variety  $V_2$  ( $P_2$ ), respectively, plotted against local aggregation. Fields with the variety  $V_1$  are displayed in red, those with variety  $V_2$  in black.

#### 4. Discussion

During both the population establishment phase and the coexistence at population equilibrium, landscape structure had a strong effect on the genetic structure of the pathogen population. Highly fragmented landscapes were found favorable to the generalist genotype. When the variety aggregation level was high (mosaic or clustered), the generalist genotype had more difficulties establishing a population but the geometry and size of the variety aggregates interacted with the initial position of inoculums to produce local populations. Such effect could give opportunities for the generalist to locally build a population. Another output of the study was that coexistence between the three genotypes occurred rather easily.

Our study is an illustration of the application of the classical theory of hard and soft selection (Christiansen, 1975; Wallace, 1975) to an epidemiological question in a spatially explicit model. Hard and soft selection theory predicts that coexistence occurs in subdivided

populations when selection is soft (*i.e.* selection occurs before dispersal) whereas when selection is hard (*i.e.* selection occurs after dispersal and then), coexistence is impossible. In our model, we expected selection to be hard (Vale, 2013) but, as previously shown by Débarre and Gandon (2011), we found that in heterogeneous environment, the selection become softer when the specialist cost is weak and when the environment heterogeneity is high. Moreover, we show that local specificity of spatial heterogeneity can create areas of soft selection enabling coexistence even when global landscape descriptors indicate hard selection. During the establishment phase, two kinds of spatial structures were obtained for the mutant population. Highly fragmented landscapes led to diffuse generalist populations, whereas higher aggregation levels of the cultivars led to the establishment of local populations. This can be of practical interest for disease management since localized populations can be controlled more easily by crop rotations or local pesticide applications (Carolan et al., 2017), while diffuse populations seem more difficult to handle. However, the establishment of large local populations of the generalist genotype makes it less susceptible to demographic or environmental stochasticity. The high variability of the size of the mutant population was also discussed by Burton and Travis (2008). They found substantial variation in the fate of mutations depending on where they arise in space during the population expansion, in particular when corridor structures were present in the landscape. Corridor structures tended to slow down the resident population and so allowed the mutant population to get locally established through foundation effects. Our model also produced similar effects. On the contrary to Burton and Travis (2008), we considered a resident population composed by two genotypes each one specialized on one variety. In addition to the interaction between landscape structure and initial position of inoculums, there was also a strong effect of the relative position of initial inoculum of each genotype. Given that mutants appear at the highest frequency in the most diseased areas, then in direct competition with wild types, the establishment of a mutant population seems not easy

to obtain (Wei and Krone, 2005). Our study suggests that spatial local structures of the cultivated landscape play a crucial role in allowing the establishment of mutant populations. Such effects are probably extremely difficult to control by crop management strategies.

Hallatschek and Nelson (2009) developed and analyzed a model that described the population dynamics and the genetic segregation on expanding microbial colonies. They proposed several relationships between the observed genetic patterns and the selective advantage / disadvantage of mutations. As an example, they showed that beneficial mutations give rise to sectors with an opening angle that depends on the selective advantage of the mutants. However, they did not consider heterogeneous environments. In our case, we were able to provide some relationship between landscape structure and observed pathogen genetic patterns. Nevertheless, the description of the structure of the pathogen genetic pattern and the shape of the variety aggregates needs to go further in order to extract as much information as possible on which landscape structure, in interaction with the initial position of inoculum, gives rise to which spatial pattern of the mutant population (Möbius et al., 2015).

After the establishment phase, at the population equilibrium, the coexistence among pathogen genotypes was highly stable between landscape structures, as long as the variety proportions and aggregation level and the spore dispersal range did not vary. In accordance with Débarre and Lenormand (2011), we found that habitats boundaries provide opportunities for the generalist genotype to persist in the landscape. In our study, however, the ‘habitat boundary polymorphism’ acted within a more flexible framework, including complex landscape structures, an explicit life-cycle and stochasticity in the pathogen life events. In addition, it was also possible to observe coexistence among the three pathogen genotypes in a quasi-neutral model, *i.e.* when dispersal scale was high, aggregation was low and the varieties were in balanced proportions. Habitat boundaries are highly diversified zones. In agro-ecosystems, particular boundaries are those between production and natural components of

agricultural landscapes. It is recognized that the agro-ecological interface significantly influences disease dynamics and evolution of plant pathogen (Burdon and Thrall, 2008; Papaix et al., 2015). Agro-ecosystems provide a range of situations including both agricultural crops and wild reservoirs. Our study highlights the importance of borders as a diversity reservoir contributes to answering the question of the effect of the agro-ecological interface on evolutionary changes in plant pathogens.

Our study shows that the structure of cultivated landscapes, in terms of cultivar composition and spatial distribution, influences the probability for mutant population establishment. It also shows that local structures may have great consequences by allowing a mutant population to establish. Even though such a population is restricted to a small area, it may persist and spread over the years, depending of the changes in the host population. We described here the competition between generalist and specialist pathogen genotypes. In order to interpret the results for crops health management, one has to decide which of the generalist or the specialist is the less damaging for the crops. This is not a trivial question and probably depends on the context. In most cases, diversification schemes aiming at the control of epidemics are based on the mixtures of varieties with major resistance genes that will discriminate compatible (or virulent) stains among the pathogen population. Typically this is the case of variety mixtures (Mundt, 2002) but the idea has been extended to the landscape scale (Brophy and Mundt, 1991; Zhu et al., 2000; Papaix et al., 2018). This kind of strategy is based on the idea that specialists will develop less damaging epidemics in a diversified environment, due to dilution effects (Keesing et al., 2006). In that case, a generalist pathogen becomes a problem and the diversification strategy has to be adapted to avoid the establishment and development of a generalist population (Lannou and Mundt, 1997). A different context is the introduction of a new cultivar in a cultivated landscape confronted to an already diversified pathogen population. A population study on leaf rust of wheat in France showed that quantitative differences in

pathogenicity among pathogen - host genotype combinations accounted for the pathogen population structure and distribution over the host varieties as well as the disease levels on the different host varieties (Papaix et al., 2011). Moreover, this population analysis exemplified how a specialist pathogen could produce devastating epidemics on a susceptible host, whereas generalist pathogens, less pathogenic, remained less damaging.

There is probably no absolute answer to the question of whether specialist or generalist pathogens are more damaging for crops. This depends on the context, including the pathogen population structure, the host distribution, the kind of resistance genes involved (qualitative or quantitative resistance, or both), etc. This paper does not give a direct answer on how to deploy varieties in an agricultural landscape but rather indications on the different effects that should be considered, and their possible consequences.

## 5. References

- B Barrès, F Halkett, C Dutech, A Andrieux, J Pinon, and P Frey. Genetic structure of the poplar rust fungus *melampsora larici-populina*: evidence for isolation by distance in europe and recent founder effects overseas. *Infection, Genetics and Evolution*, 8: 577–587, 2008.
- A Bouvier, K Kiêu, K Adamczyk, and H Monod. Computation of the integrated flow of particles between polygons. *Environmental Modelling & Software*, 24: 843–849, 2009.
- L S Brophy and C C Mundt. Influence of plant spatial patterns on disease dynamics, plant competition and grain yield in genetically diverse wheat populations. *Agriculture, Ecosystems and Environment*, 35: 1–12, 1991.
- J J Burdon and P H Thrall. Pathogen evolution across the agro-ecological interface: Implications for disease management. *Evolutionary Applications*, 1: 57–65, 2008.
- O J Burton and J M J Travis. Landscape structure and boundary effects determine the fate of mutations occurring during range expansions. *Heredity*, 101: 329–340, 2008.

K Carolan, J Helps, F van den Berg, R Bain, N Paveley, and F van den Bosch. Extending the durability of cultivar resistance by limiting epidemic growth rates. *Proceedings of the Royal Society (B)*, 284: 20170828, 2017.

P Chesson. Mechanisms of maintenance of species diversity. *Annual Review of Ecology and Systematics*, 31: 343–366, 2000.

Freddy Bugge Christiansen. Hard and soft selection in a subdivided population. *The American Naturalist*, 109: 11–16, 1975.

B C Couch, I Fudal, M-H Lebrun, D Tharreau, B Valent, P van Kim, J-L Nottoghem, and L M Kohn. Origins of host-specific populations of the blast pathogen *Magnaporthe oryzae* in crop domestication with subsequent expansion of pandemic clones on rice and weeds of rice. *Genetics*, 170: 613–630, 2005.

F Débarre and S Gandon. Evolution in heterogeneous environments, between soft and hard selection. *The American Naturalist*, 177: E83–E97, 2011.

F Débarre and T Lenormand. Distance-limited dispersal promotes coexistence at habitat boundaries: reconsidering the competitive exclusion principle. *Ecology Letters*, 14: 260–266, 2011.

L Excoffier and N Ray. Surfing during population expansions promotes genetic revolutions and structuration. *Trends in Ecology and Evolution*, 23: 347–351, 2008.

H H Flor. Current status of the gene-for-gene concept. *Annual Review of Phytopathology*, 9: 275–296, 1971.

P R Gérard, C Husson, J Pinon, and P Frey. Comparison of genetic and virulence diversity of *Melampsora larici-populina* populations on wild and cultivated poplar and influence of the alternate host. *Phytopathology*, 96: 1027–1036, 2006.

A J Gibbs, K Ohshima, M J Phillips, and M J Gibbs. The prehistory of potyviruses: Their initial radiation was during the dawn of agriculture. *PLoS ONE*, 3: e2523, 2008.



P Gladieux, X G Zhang, I Roldan-Ruiz, V Caffier, T Leroy, M Devaux, S Van Glabeke, E Coart, and B Le Cam. Evolution of the population structure of *venturia inaequalis*, the apple scab fungus, associated with the domestication of its host. *Molecular Ecology*, 19: 658–674, 2010.

H Goyeau, R Park, B Schaeffer, and C Lannou. Distribution of pathotypes with regard to host cultivars in French wheat leaf rust populations. *Phytopathology*, 96: 264–273, 2006.

O Hallatschek and D R Nelson. Life at the front of an expanding population. *Evolution*, 64: 193–206, 2009.

A P Hendry, T J Farrugia, and M T Kinnison. Human influences on rates of phenotypic change in wild animal populations. *Molecular Ecology*, 17: 20–29, 2008.

M S Hovmoller, L Munk, and H Ostergard. Observed and predicted changes in virulence gene-frequencies at 11 loci in a local barley powdery mildew population. *Phytopathology*, 83: 689–689, 1993.

T Johnson. Man-guided evolution in plant rusts. *Science*, 10: 357–362, 1961.

F Keesing, R D Holt, and R S Ostfeld. Effects of species diversity on disease risk. *Ecology Letters*, 9: 485–498, 2006.

K Kiêu, K Adamczyk-Chauvat, H Monod, and R S Stoica. A completely random T-tessellation model and Gibbsian extensions. *Spatial Statistics*, 6: 118–138, 2013.

C Lannou. Variation and selection of quantitative traits in plant pathogens. *Annual Review of Phytopathology*, 50: 319–338, 2012.

C Lannou and C C Mundt. Evolution of a pathogen population in host mixtures: rate of emergence of complex races. *Theoretical Applied Genetic*, 94: 991–999, 1997.

B A Melbourne, H V Cornell, K F Davies, C J Dugaw, S Elmendorf, A L Freestone, R J Hall, S Harrison, A Hastings, M Holland, M Holyoak, J Lambrinos, K Moore, and H Yokomizo.

Invasion in a heterogeneous world: Resistance, coexistence or hostile takeover? *Ecology Letters*, 10: 77–94, 2007.

W Möbius, A W Murray, and D R Nelson. How obstacles perturb population fronts and alter their genetic structure. *PLOS Computational Biology*, 11: e1004615, 2015.

C C Mundt. Use of multiline cultivars and cultivar mixtures for disease management. *Annual Review of Phytopathology*, 40: 381–410, 2002.

C C Mundt, K E Sackett, L D Wallace, C Cowger, and J P Dudley. Long-distance dispersal and accelerating waves of disease: Empirical relationships. *The American Naturalist*, 173: 456–466, 2009.

A B Munkacsı, S Stoxen, and G May. *Ustilago maydis* populations tracked maize through domestication and cultivation in the americas. *Proceedings of the Royal Society B*, 275: 1037–1046, 2008.

S R Palumbi. Evolution - humans as the world’s greatest evolutionary force. *Science*, 293: 1786–1790, 2001.

J Papaix, H Monod, H Goyeau, P du Cheyron, and C Lannou. Influence of cultivated landscape composition on variety resistance: An assessment based on wheat leaf rust epidemics. *New Phytologist*, 191: 1095–1107, 2011.

J Papaix, K Adamczyk-Chauvat, A Bouvier, K Kiêu, S Touzeau, C Lannou, and H Monod. Pathogen population dynamics in agricultural landscapes: The Ddal modelling framework. *Infection, Genetics and Evolution*, 27: 509–520, 2014.

J Papaix, J J Burdon, J S Zhan, and P H Thrall. Crop pathogen emergence and evolution in agro-ecological landscapes. *Evolutionary Applications*, 8: 385–402, 2015.

J Papaix, L Rimbaud, J J Burdon, J Zhan, and P H Thrall. Differential impact of landscape-scale strategies for crop cultivar deployment on disease dynamics, resistance durability and long-term evolutionary control. *Evolutionary Applications*, 11: 705–717, 2018.

B Pariaud, V Ravigné, F Halkett, H Goyeau, J Carlier, and C Lannou. Aggressiveness and its role in the adaptation of plant pathogens. *Plant Pathology*, 58: 409–424, 2009.

R Core Team. *R: A Language and Environment for Statistical Computing*. R Foundation for Statistical Computing, Vienna, Austria, 2018. URL <https://www.R-project.org/>.

T Rouxel, A Penaud, X Pinochet, H Brun, L Gout, R Delourme, J Schmit, and M H Balesdent. A 10-year survey of populations of *Leptosphaeria maculans* in France indicates a rapid adaptation towards the Rlm1 resistance gene of oilseed rape. *European Journal of Plant Pathology*, 109: 871–881, 2003.

S Soubeyrand, I Sache, C Lannou, and J Chadoeuf. A frailty model to assess plant disease spread from individual count data. *Journal of Data Science*, 5: 67–83, 2007.

E H Stukenbrock and B A McDonald. The origins of plant pathogens in agro-ecosystems. *Annual Review of Phytopathology*, 46: 75–100, 2008.

E H Stukenbrock, S Banke, M Javan-Nikkhah, and B A McDonald. Origin and domestication of the fungal wheat pathogen *mycosphaerella graminicola* via sympatric speciation. *Molecular Biology and Evolution*, 24: 398–411, 2007.

P F Vale. Killing them softly: managing pathogen polymorphism and virulence in spatially variable environments. *Trends in parasitology*, 29: 417–422, 2013.

W N Venables and B D Ripley. *Modern Applied Statistics with S*. Springer, New York, fourth edition, 2002. ISBN 0-387-95457-0.

B Wallace. Hard and soft selection revisited. *Evolution*, 29: 465–473, 1975.

W Wei and S M Krone. Spatial invasion by a mutant pathogen. *Journal of Theoretical Biology*, 236: 335–348, 2005.

KA With. The landscape ecology of invasive spread. *Conservation Biology*, 16: 1192–1203, 2002.

M S Wolfe and E Schwarzbach. Patterns of race changes in powdery mildews. *Annual Reviews of phytopathology*, 16: 159–180, 1978.

S N Wood. Fast stable restricted maximum likelihood and marginal likelihood estimation of semiparametric generalized linear models. *Journal of the Royal Statistical Society (B)*, 73: 3–36, 2011.

Y Zhu, H Chen, J Fan, Y Wang, Y Li, J Chen, J X Fan, S Yang, L Hu, H Leung, T W Mew, P S Teng, Z Wang, and C C Mundt. Genetic diversity and disease control in rice. *Nature*, 406: 718–722, 2000.